

# Design Specifications and Optimisation of a Directly Grid-Connected PM Wind Generator

Johannes H. J. Potgieter, *Student Member, IEEE* and Maarten J. Kamper, *Senior Member, IEEE*

Department of Electrical and Electronic Engineering

Stellenbosch University

Stellenbosch, South Africa

Email: kamper@sun.ac.za

**Abstract**—This paper forms part of a broader study on the design and implementation of a slip-synchronous permanent magnet wind generator. This is a gearless, direct-drive generator connected directly to the utility grid without a power electronic converter. The system consists of two integrated generating units, a directly turbine connected slip permanent magnet generator and a conventional grid-connected permanent magnet synchronous generator. The focus of this study is to define the exact design requirements of the directly grid connected synchronous generator unit from the relevant grid code specifications, and to find the optimum design subject to these requirements. Due to the direct grid connection there are clear differences in the design requirements of this machine and those of conventional PM wind generators connected to the grid via a converter. Different generator topologies are evaluated with regard to ease of manufacturing, active mass, PM content and suitability for direct grid connection. Simulation results are presented and measured results are given for an existing directly grid-connected PM generator to confirm the FE-calculations.

## I. INTRODUCTION

In order to increase the competitiveness of wind energy generation, operation and maintenance costs are very important considerations in the implementation of wind generating systems. Especially for systems with limited access, such as offshore turbines it is essential that operation and maintenance is reduced to a minimum. At present, most installed systems make use of a doubly-fed induction generator (DFIG), with a gearbox and partially rated power electronic converter. Due to gearbox failures owing to high financial implications, direct-drive, gearless PM generators connected to the grid via a full rated power electronic converter are considered in new installations as well. However, due to the current high cost of PM material, synchronous generators with wound rotors and smaller medium speed PM generators operated with a gearbox having a lower gearing ratio, are also considered. Although not as severe as gearbox failures and with components easier to replace, electrical failures are the most common type of failure for wind generator systems. Thus, it is clear that if the gearbox and power electronic converter is removed from the drive train the reliability of wind turbine systems can be increased significantly. An electrical machine capable of operating without a gearbox or power electronic converter in a wind generator setup is the permanent magnet induction generator (PMIG). The concept was first introduced by [1] in 1926. Initially the PMIG was proposed to improve the power factor of conventional induction machines, with later studies, as in [2] and [3], proposing it for use as a direct-drive,

directly grid connected PM wind generator. Due to the PMIG being a fixed speed system it is also proposed as a doubly fed generator with a partially rated converter in [4] which allows some margin of speed control. In [5] it is proposed that several PMIGs be connected in a common grid of which the voltage and frequency is controlled by a single converter to allow for variable speed operation. Several other studies exist on this concept, with the contribution of each of the relevant literature works thoroughly discussed in [6].

The slip synchronous permanent magnet generator (SS-PMG) that was recently introduced in [6] is based upon the PMIG concept, with the difference being that the stator and slip-rotor windings are electromagnetically separated. The SS-PMG consists of two integrated generating units, a slip permanent magnet generator (slip-PMG) which is fixed to the turbine and a permanent magnet synchronous generator (PMSG) directly grid connected. These generating units are mechanically linked by a common PM-rotor with separate sets of PMs for each. A cross-section diagram and example of a SS-PMG are shown in Fig. 1(a) and (b). A voltage is induced in the windings of the slip-PMG at slip frequency and in the PMSG at synchronous frequency as explained in the equivalent circuit of the SS-PMG in Fig. 1(c). The evaluation and optimum design of the slip-PMG unit is thoroughly covered in [7]. The focus of this paper is, thus, on the optimum design of the PMSG unit. Although the PMSG unit is similar to conventional PM generators connected to the grid via a power electronic converter of which the design optimisation is well known, [8] and [9], there are different design requirements due to this generator being directly grid-connected.

Although limited and only conceptual there are other studies mentioned in literature on directly grid connected PM synchronous wind generators. In [10] a spring and damper system are used to damp power angle oscillations of a directly grid-connected PMSG. There are also the directly grid-connected synchronous generator concepts where the generator is connected to the turbine via a hydro-dynamically controlled gearbox with a fixed speed output and variable speed input. An example of such a system is discussed in [11], where an in depth study is done regarding the grid connection aspects of this generator. Several favourable grid connection characteristics are mentioned, such as that the directly grid connected synchronous generator can provide the highest amount of reactive power support with regard to other wind generator topologies. Another directly grid connected PM generator concept is as proposed in [12] where a partially rated converter is placed in the star point of the generator to damp oscillations

resulting from load variations. However, no clear indication can be found in the literature on the exact design requirements of the directly grid-connected PM wind generator.

Four different generator topologies are considered in the design optimisation namely, mass, PM content and ease of manufacturing such as is generally the case for the design of PM wind generators. Very important also is the suitability of the different designs for direct grid connection. Due to practical considerations a 15 kW directly grid-connected SS-PMG system is used as a case study and for measurements. Optimum finite element (FE) designs are given for four different PM generator topologies.

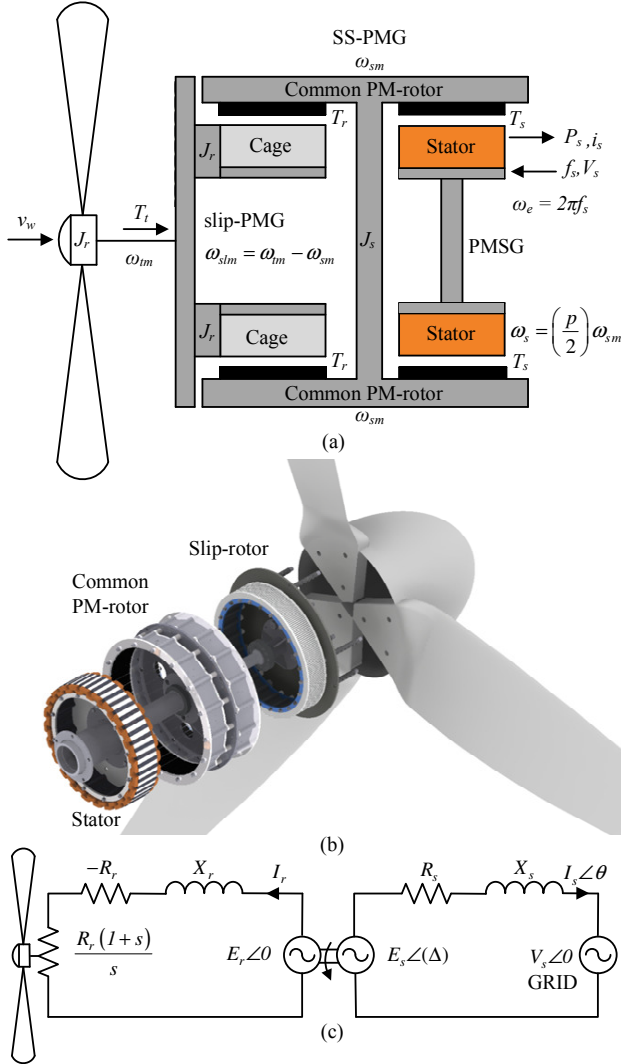


Fig. 1. (a) SS-PMG cross section diagram, (b) complete prototype SS-PMG wind turbine system and (c) equivalent circuit [6].

## II. DESIGN SPECIFICATIONS

The design aspects of the directly grid connected SS-PMG are assessed in two parts in this section. First the relevant grid code specifications are summarised and secondly the requirements for the specific turbine system and direct-drive wind generators in general are discussed. Furthermore, the

whole aim of the SS-PMG is to have an as simple and robust as possible wind generator system. This design methodology is, thus, applied throughout the whole generator design process.

### A. Direct Grid Specifications

For this study the local applicable grid-codes and regulations for wind turbine facilities are used as a basis to obtain the design specifications of the generator as stipulated in [13], [14] and [15]. The SS-PMG is synchronised to the grid by means of a grid-synchronisation controller as explained in [16]. For utility scale systems an electronically controlled tap-changing transformer configuration is proposed to monitor and change the terminal voltage at the point of common coupling (PCC) as required by the utility and as explained in [17]. In [18] the low voltage ride through (LVRT) capabilities of the SS-PMG are evaluated. The systems as mentioned above are responsible for the implementation of the grid code requirements. However, it is still necessary that the generator design complies with many of the aspects listed below and also discussed in [16] - [18]:

- The power factor (PF) should not be less than 0.975 leading or lagging for systems < 20 MW, > 0.95 for systems > 20 MW and > 0.9 for small scale systems.
- In some cases active power control is needed, especially during grid frequency variations, to reduce the power delivered to the grid.
- In many cases it is essential to control the reactive power delivered to or absorbed from the grid and the power factor at the PCC. Regarding small scale generation, under no circumstances may reactive power be injected into the grid.
- Reactive power and voltage should be controlled with a tolerance of 0.5 % of the rated power.
- The system needs to be able to operate in a voltage range of  $\pm 10$  % around the nominal voltage at the PCC continuously.
- The system should stay connected to the grid during low voltage and over voltage conditions as stipulated by the regimes shown in [13].
- Frequency variations between 47 Hz and 52 Hz at a rate of change of 0.5 Hz/s needs to be accommodated.
- The quality of the power delivered should comply to the limits set in [14]. Individual levels are provided for the different harmonic orders and a total harmonic distortion (THD) level of 8 % is given. In [15] a THD of 5 % is mentioned for small scale systems.

### B. Design Issues in General

Direct-drive PM wind generators are heavy with high quantities of PM material to produce the torque required. Furthermore, these generator types are the most expensive drive-train solution currently in use, as explained in [8]. Hence, for the design of PM generators, aspects need to be addressed such as the mass of the generator, the PM content, efficiency, load torque ripple and especially the no-load cogging torque, ease of manufacturing, segmentation of the generator and cost [9]. For the 15 kW case study system under consideration Table I gives some of the constraints associated with this design.

From the turbine curves for the 15 kW wind generator system to be implemented, a rated torque value of  $T_r = 1000$

TABLE I. DESIGN CONSTRAINTS OF THE 15 kW CASE STUDY SS-PMG SYSTEM.

Parameter	Value
Rated torque, $T_{rated}$ , Nm	1000
Maximum breakdown torque $T_b$ , pu	$\geq 2.0$
No-load cogging torque, $\Delta\tau_{NL}$ , %	$\leq 2.5$
Full-load torque ripple, $\Delta\tau_L$ , %	$\leq 4.0$
Required rated efficiency, $\eta_s$ , %	$\geq 94$
Maximum outer diameter, $D_o$ , mm	655
Minimum wind speed, $v_{min}$ , m/s	4
Rated wind speed, $v_w$ , m/s	11
Rated rotor speed $n_s$ , r/min	150
Grid line voltage $V_s$ , V	400
Grid frequency $F_s$ , Hz	50

Nm, at a rated turbine speed of  $n_s = 150 \text{ r}\cdot\text{min}^{-1}$ , and rated wind speed of  $v_w = 11 \text{ m/s}$  is selected. From the dimensions of the evaluated turbine, the maximum outer diameter of the generator is fixed at  $D_o = 655 \text{ mm}$ . Normally for utility scale systems making use of mechanical and aerodynamic braking the maximum torque seldom exceeds a value  $T_b \geq 1.5 \text{ pu}$ . However, for the 15 kW fixed-pitch system under consideration, electromagnetic braking is employed and in this case the maximum torque is specified as  $T_b \geq 2.0 \text{ pu}$  [19]. From previous studies such as the design in [20], a no-load cogging torque value of  $\Delta\tau_{NL} \leq 2.5\%$  and a load torque ripple of  $\Delta\tau_L \leq 4\%$  are specified. In some cases a cogging torque value even as low as  $\Delta\tau_{NL} \leq 0.5\%$  is mentioned, but for this study the given value is deemed sufficient in order to obtain a fair comparison between the different generator systems evaluated. With the efficiency of the slip-PMG unit given as  $\eta_r = 97\%$  in [7] and to have an overall system efficiency of  $\eta_t = \eta_s\eta_r \geq 91\%$ , the efficiency of the PMSG should be no less than  $\eta_s \geq 94\%$ . It is also essential that the partial load efficiency be adequately evaluated as this is the region in which the wind generator will be operated most of the time. Furthermore, the short-circuit current level needs to be limited during low voltage conditions to limit damage to switch gear and transformers and also to protect the PMs from demagnetisation.

### III. GENERATOR TOPOLOGIES CONSIDERED

For this study both non-overlap single layer (SL) and double layer (DL) windings as shown in Fig. 2(a) and (b) respectively, are evaluated. Furthermore, in this study a new type of toroidal winding is also considered as shown in Fig. 2(c). Next to each machine structure the slot layout with regard to the different phases are shown. For comparison the phase layout of a SL and DL conventional three phase overlap winding making use of three slots per pole are also shown in Fig. 2(d). The toroidally wound machine makes use of six slots per pole.

Non-overlap winding PM machines have the advantages of easier manufacturing and segmentation as well as low cogging torque. The number of coils for the same pole number is also much lower and pre-formed windings can easily be used by slightly adjusting the slot-layout. This is even easier if a SL non-overlap winding, where each alternating tooth is wound, is utilised and the amount of coils are also halved as opposed to the DL winding. However, the drawbacks of the SL non-overlap winding as shown in previous studies is the large sub-MMF harmonic [20]. It is also known that the voltage quality of the SL winding is poorer than that of the DL winding. As

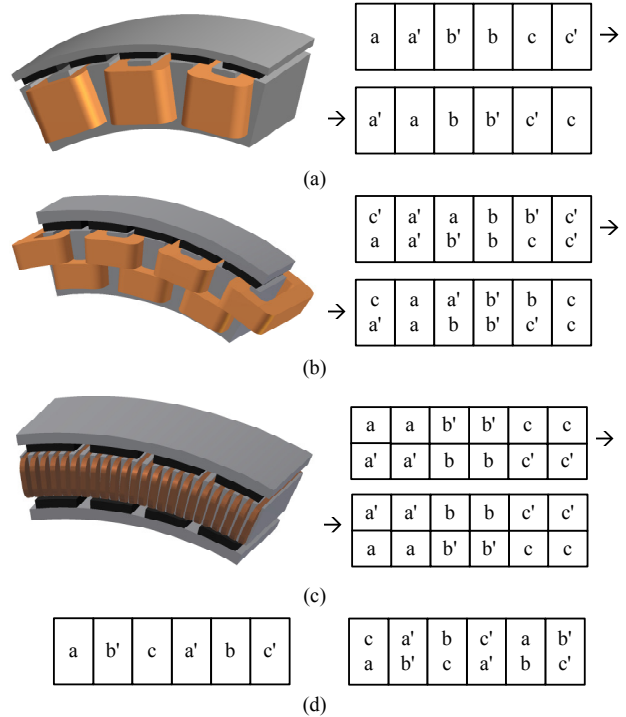


Fig. 2. (a) Non-overlap SL and (b) DL, (c) double-rotor toroidal 6 slot/pole PMSG winding structures and phase layouts and (d) conventional three phase overlap winding SL and DL phase layouts.

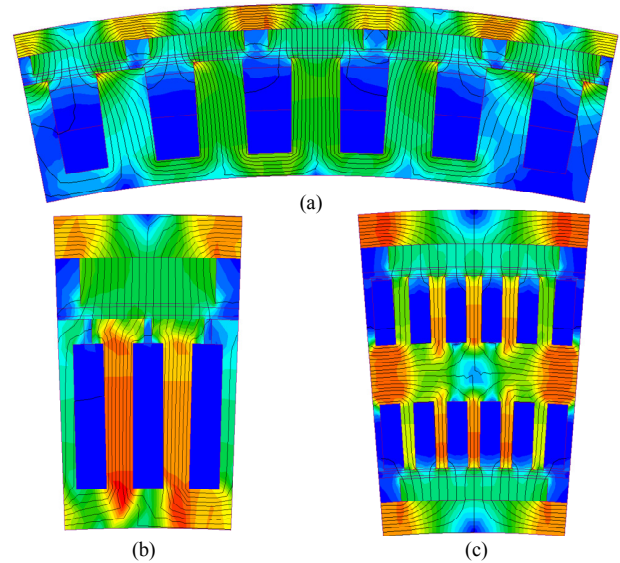


Fig. 3. FE field plots for the (a) Non-overlap DL, (b) conventional three phase overlap winding and (c) double-rotor toroidal 6 slot/pole PMSGs.

for the design of the slip-PMG unit as in [7], the DL winding is also found to have a better performance than that of the SL non overlap winding machine. As opposed to the double layer winding configuration shown in Fig. 2(b) the coils can be placed adjacent to one another instead of stacked on top of one another. This will make segmentation of the non overlap DL winding easier. Fig. 3(a) shows a FE field plot of the DL

non-overlap winding PM machine.

Overlap winding machines on the other hand are known to have a much better torque performance and should, thus, require less active and PM material for the same torque specifications. These machines, however, have the problem of a very large torque ripple and a high number of coils. On the other hand the overlap winding machine makes use of a conventional three phase winding for which commercial winding processes have been available for a long time. A known problem for especially larger powers, though, is the segmentation of the stator winding. The large end-windings could also be a problem especially for machines with short axial lengths, typical of direct-drive wind generators. There are also questions regarding the effects of the known very low per unit impedance of these machines for direct grid connection. In Fig. 3(b) a FE simulated flux plot of a conventional overlap winding PM machine with three slots per pole is shown.

Dual rotor PM machine topologies have been proposed for both overlap and non overlap windings. However, in the case of overlap winding machines, the large end-windings could make it difficult to assemble the machine, which means that the eventual configuration might not be at the optimum machine dimensions. In this case it might be better to go for the toroidal type of topology such as in [21] and [22]. Normally toroidally wound coils are wound around a steel cylinder with the stator being toothless. This allows for easier manufacturing but the drawback is a large airgap that requires more PM material. In this study a slotted stator configuration is used with slots on both the inner and outer diameters of the stator, as shown in Fig. 2(c) and Fig. 3(c) which shows the FE field plot of the toroidal winding machine. The machine is assembled in such a way that two opposing magnet polarities are facing one another. The flux from the bottom magnet, thus links the bottom conductor and the flux from the top magnet links the top conductor. Currently it is difficult to comment on the manufacturability of the double rotor toroidal winding as this type of winding has not been extensively used before, especially for large diameter wind turbines. However, segmentation for this type of winding should not be a problem due to none of the coils overlapping. For all the configurations in Fig. 3 negative boundary conditions are used in the FE analysis.

#### IV. DESIGN METHODOLOGY

As mentioned in [6] it is not possible to know the operating state of the directly grid connected PMSG as the current angle cannot be controlled as is the case for a PMSG connected to the grid via a solid-state converter. A special type of simulation procedure is, thus, required in conjunction with the design equations presented in this section. This procedure is thoroughly discussed in [6].

##### A. Design Equations

The directly grid-connected PMSG is modelled in the  $dq$ -reference frame fixed to the PM-rotor. From the  $dq$ -equivalent circuits in Fig. 4 the steady-state  $dq$ -equivalent equations are given as

$$V_q = -R_s I_q - \omega_s (L_d + L_e) I_d + \omega_s \lambda_m \quad (1)$$

and

$$V_d = -R_s I_d + \omega_s (L_q + L_e) I_q. \quad (2)$$

$V_d$  and  $V_q$  and  $I_d$  and  $I_q$  indicate the  $d$  and  $q$ -axis voltages and currents respectively.  $R_s$  is the per phase resistance and  $\omega_s = 2\pi f_s$  indicates the synchronous electrical angular speed. The  $dq$ -inductances  $L_d$  and  $L_q$  are given as

$$L_q = \frac{\lambda_q}{-I_q}; \quad L_d = \frac{\lambda_d - \lambda_m}{-I_d}. \quad (3)$$

The end-winding inductance component is indicated by  $L_e$ , and the methods used to calculate this parameter are thoroughly discussed in [23]. It is found that end-effects of both the windings and PMs can have a significant effect on the performance of the machine especially regarding the calculation of the maximum torque and current.

The general relations of voltage and current are given from Fig. 4 by

$$\begin{bmatrix} V_q \\ V_d \end{bmatrix} = \sqrt{2} V_{rms} \begin{bmatrix} \cos \Delta \\ \sin \Delta \end{bmatrix}, \quad (4)$$

$$\begin{bmatrix} I_q \\ I_d \end{bmatrix} = \sqrt{2} I_{rms} \begin{bmatrix} \cos \alpha_s \\ \sin \alpha_s \end{bmatrix}, \quad (5)$$

$$V_q^2 + V_d^2 = 2V_{rms}^2 \quad (6)$$

and

$$I_q^2 + I_d^2 = 2I_{rms}^2. \quad (7)$$

The per phase grid voltage is fixed at  $V_{rms} = 230$  V, and the stator current fed into the grid can be calculated as

$$I_{rms}^2 = \frac{P_{cu}}{3R_s}, \quad (8)$$

with  $P_{cu}$  in (8) the copper loss of the stator winding which is given as an input parameter. The developed torque is given by

$$T_s = \frac{3}{4} p [(L_q - L_d) I_d I_q + \lambda_m I_q] \quad (9)$$

and the efficiency by

$$\eta_s = \frac{T_s \omega_{sm} - P_{Loss}}{T_s \omega_{sm}}. \quad (10)$$

The total generator losses are defined as  $P_{Loss} = P_{cu} + P_{ecs} + P_{ecr} + P_{wf}$ .  $P_{ecs}$  indicates the core losses in the stator steel.  $P_{ecr}$  includes the core losses in the rotor yoke as well as the PM eddy losses for the PM-rotor. These values are calculated by means of FE-analysis. The wind and friction losses are given by  $P_{wf}$  which is a fixed value for the fixed speed SS-PMG system. Finally the working power and reactive power supplying to or consuming from the grid is given as

$$\begin{bmatrix} P_s \\ Q_s \end{bmatrix} = 3V_{rms} I_{rms} \begin{bmatrix} \cos \theta \\ \sin \theta^* \end{bmatrix}. \quad (11)$$

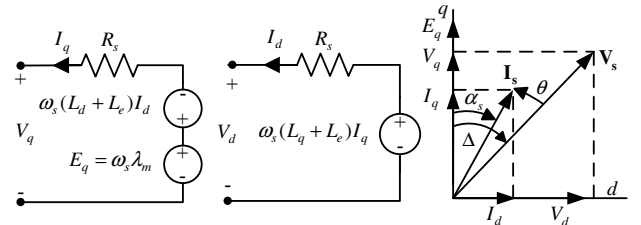


Fig. 4.  $DQ$ -equivalent circuits and vector diagram for the modelling of the direct-grid PMSG.

The maximum breakdown torque the generator is capable of can be calculated by means of the methods as explained in [7] and [19].

### B. Modelling Procedure

The equations above are now used in the static modelling procedure coupled with an optimisation algorithm as shown in Fig. 5 and thoroughly explained in [6]. The input parameters are indicated by  $\mathbf{X}$  and the output performance parameters by  $\mathbf{Y}$ . Initially the current angle is assumed as  $\alpha_s = 0$  with  $I_d = 0$ , and a first static FE iteration is solved. Initial values for the inductances can now be calculated with the assumption that  $L_d \approx L_q$ . With the inductance values known an initial value for  $\alpha_s$  can be calculated from (1) - (8). How the initial value for  $\Delta$  is chosen is explained in [6]. With the current angle and peak current for each phase known a second static FE iteration can be solved with  $L_d$  and  $L_q$  more accurately calculated in this case with (3). About three to four static FE-iterations are needed to find the operating state of the generator at which the performance is simulated using the equations above. Static FE is much faster than transient FE, which means that optimisation is much quicker. After optimisation each optimum design is verified by means of transient FE, and slight adjustments are made to  $\mathbf{X}$  so that all the performance output parameters in  $\mathbf{Y}$  comply with the limits set in Section II. The reason for transient verification is to accurately calculate the torque ripple as well as the eddy current losses, which cannot be accurately calculated by static FE. Upon completion of the FE-design iterations, a final check is done to determine if the generator design complies with the mentioned grid requirements. This is done with the help of the dynamic modelling methods as discussed in [24]. If the dynamic grid performance of the generator is not sufficient, the optimum FE-design needs to be altered. The parameters which influence the grid behaviour the most are typically the size of the synchronous reactance ( $X_s$ ), and the PM strength.

### V. OPTIMISATION RESULTS

Table II gives the optimisation results for the four PM machine topologies evaluated. An indication of the size of the machines can be found with  $l$  the active length and  $D_i$  the inside diameter. The maximum outside diameter of all the machines is fixed at 655 mm. The active mass ( $M_{Tot}$ ) of the four different generator topologies is minimised during optimisation subject to the design constraints discussed in Section II. The optimum PM mass ( $M_{PM}$ ) for each machine topology is found with the help of Fig. 6. Shown in Fig. 6 are the active mass versus PM mass curves for each of the machine topologies. About three to four optimised points subject to a certain constraint for the PM mass are shown. Each optimum point needs to comply with the design constraints given in Section II. To calculate the minimum PM mass for each generator topology, the constraint for  $M_{PM}$  is reduced until the optimised structure no longer complies with the relevant specifications.

From Table II it is seen that the two non overlap winding machines and the conventional three phase overlap winding topology have more or less the same active mass, but with the optimum PM mass of the DL non overlap winding at a slightly lower value. The double rotor toroidal winding on the other hand has a significantly lower active mass and lower

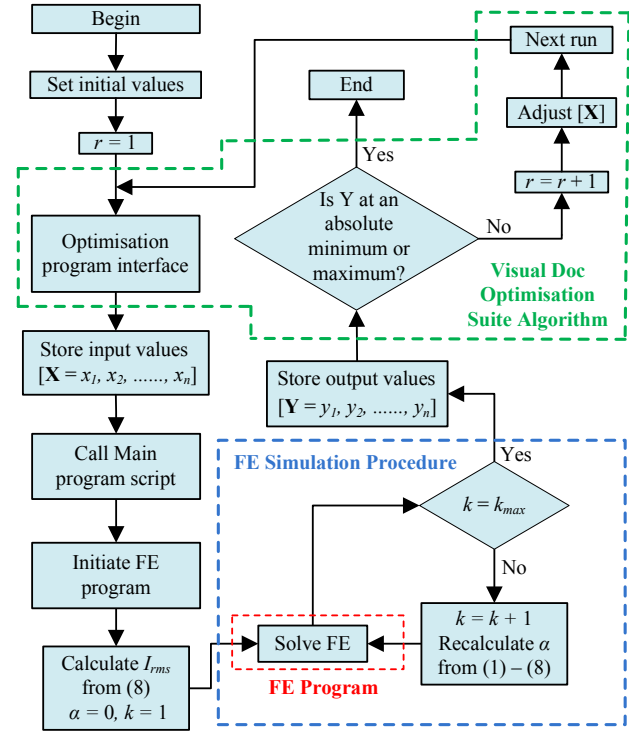


Fig. 5. Optimisation program coupled with the simulation procedure and FE simulation program.

TABLE II. OPTIMISATION RESULTS OF THE NON OVERLAP SL AND DL, CONVENTIONAL THREE PHASE OVERLAP AND DOUBLE ROTOR TOROIDALLY WOUND PMSGs.

	SL-non-overlap	DL-non-overlap	3 $\phi$ -overlap	Toroidal
$T_{rated}$ , Nm	1000	1000	1000	1000
$T_b$ , pu	2.22	2.16	3.11	4.40
$\Delta\tau_{NL}$ , %	1.90	2.34	13.37	2.35
$\Delta\tau_L$ , %	4.55	3.42	31.52	4.93
$P_{ecs}$ , W	135.36	141.39	182.37	164.56
$P_{ecr}$ , W	81.23	110.8	35.73	9.99
$P_{cu}$ , W	604.18	588.48	683.78	711.71
$\eta_s$ , W	94.57	94.44	94.01	94.00
$D_o$ , mm	655	655	655	655
$l$ , mm	129.0	125.0	114.5	80.00
$D_i$ , mm	540.1	528.0	523.2	512.0
$V_{rms}$ , V	230.0	230.0	230.0	230.0
$I_{rms}$ , A	21.93	22.64	23.70	23.80
$\Delta$ , °	12.50	12.30	10.40	6.80
$X_s$ , pu	0.247	0.208	0.082	0.068
PF	0.964	0.974	0.996	0.997
$M_{PM}$ , kg	7.62	7.00	7.82	6.49
$M_{Cu}$ , kg	16.69	20.16	25.22	21.04
$M_{Fe}$ , kg	66.37	62.44	60.77	45.22
$M_{Tot}$ , kg	90.68	89.61	93.91	71.43

**SL non overlap:** High active mass and PM content. Very easy manufacturing. Moderate to easy reduction of torque ripple. Low to moderate grid current harmonic content. High short circuit current. Moderate response to grid voltage variations.

**DL non overlap:** High active mass and moderate PM content. Easy manufacturing. Easy reduction of torque ripple. Low to moderate grid current harmonic content. High short circuit current. Moderate response to grid voltage variations.

**3- $\phi$  overlap:** High active mass and moderate PM content. Moderate to difficult manufacturing. Very high torque ripple. High grid current harmonic content. Extremely high short circuit current. Large unwanted reactive power flow if grid voltage varies from design value.

**Double rotor toroidal:** Low active mass and PM content. Moderate to difficult manufacturing. Moderate to easy reduction of torque ripple. High grid current harmonic content. Extremely high short circuit current. Large unwanted reactive power flow if grid voltage varies from design value.

optimum PM mass than the rest of the generator topologies. The minimum value of  $M_{PM}$  for the conventional overlap winding and that of the double rotor toroidal winding are both lower than that of the rest of the machine structures. This is due to the much better torque performance of these machines, with the maximum breakdown torque of the overlap winding more than 3 pu, and more than 4 pu for the double rotor toroidal winding. The rated torque of 1000 Nm is used as the base value. The reason for the much better performance regarding active mass of the toroidal winding machine compared to the conventional overlap winding machine is due to the much shorter end-windings of this winding configuration. In order to reduce the effect of the end-windings the active length is also much longer of the conventional overlap winding machine. Due to the non overlap winding machines having a much higher per unit impedance it is much more difficult for these machines to achieve the required maximum torque of  $T_b > 2.0$  pu. This is why the tendency of these machines during the design optimisation is to increase the stator inner diameter in order to decrease the steel flux path reducing the inductance of the machine. To achieve the required efficiency the active length then needs to be increased.

Regarding the direct grid connection of these different types of machines there are also other aspects which need to be addressed such as discussed previously in this paper. This relates to the power factor of the machine, harmonic content of the current waveform and the low voltage ride through capabilities. The power factor and reactive power consumption of all the topologies depend very much on the terminal voltage. It is evident that the overlap and toroidal winding machines operate at almost unity power factor. Due to the lower value of the per unit impedance  $X_s$  this generator is more sensitive to grid voltage variations and also has a higher short-circuit current. For even small variations in the terminal voltage large unwanted reactive power flow can occur. As seen in the next section both of these winding type machines, especially the conventional overlap winding machine, have a much higher harmonic content in the waveform of the current. Both these machines will, thus, need to be operated in conjunction with an additional series line reactance (SLR), which is not uncommon in power systems. The much better performance of the double-rotor toroidal winding needs to be weighed up against issues such as ease of manufacturing and the suitability of this generator for direct grid connection.

The results shown in Fig. 7 for different efficiencies and

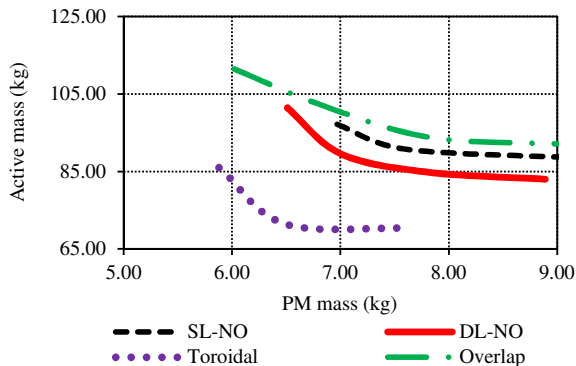


Fig. 6. PM mass versus active mass for the four PMSG machine topologies evaluated.

maximum torque specification of the DL non overlap winding machine are very interesting. When increasing the minimum efficiency from 94 % to 95 %, no major increase in mass is observed. However, when decreasing the maximum torque requirement from  $T_b > 2.0$  pu to  $T_b > 1.5$  pu, a significant reduction in mass is seen. This also explains the slightly higher efficiencies of the non overlap winding machines in Table II as the maximum torque requirement for the non overlap winding machines is a much more difficult parameter to comply with than the specified minimum efficiency. The relationship between active mass and PM content versus efficiency are shown for the double-rotor toroidally wound machine in Fig. 8. Only a marginal increase in active mass and PM content is observed when changing the minimum efficiency specification from  $\eta_s > 93$  % to  $\eta_s > 94$  %. However, for  $\eta_s > 95$  % a significant increase in active mass and PM content is observed.

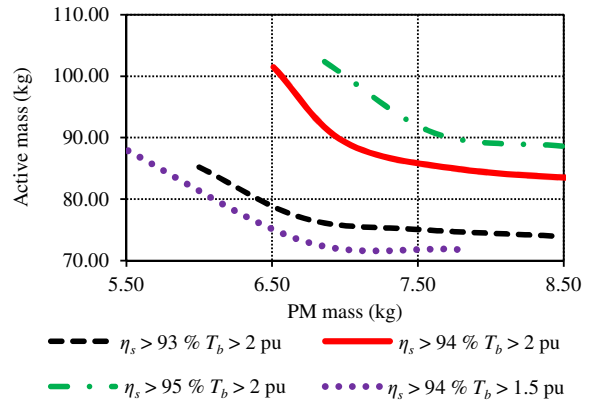


Fig. 7. PM mass versus active mass for four different design cases of the DL-non overlap winding PMSG.

## VI. MACHINE PERFORMANCE RESULTS

Fig. 9 shows the installed 15 kW directly grid connected SS-PMG wind turbine system. The grid connected stator makes use of a non overlap SL winding. The measured line current of the SL non overlap winding machine and the FE simulated line current of the toroidal wound double rotor machine fed into the grid at rated load is shown in Fig. 10. Fig. 11 shows the measured grid line voltage and the FE simulated open

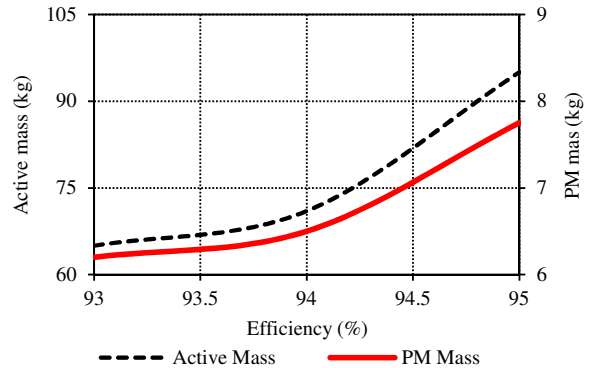


Fig. 8. PM - and active mass versus efficiency of the toroidally-wound double-rotor PMSG.



Fig. 9. Field testing of the 15 kW directly grid connected SS-PMG wind turbine system.

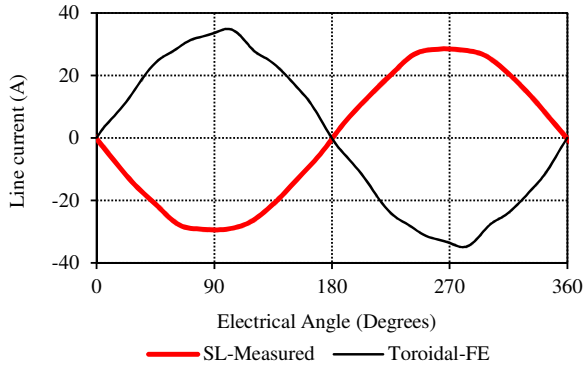


Fig. 10. Measured grid current for the SL non overlap winding machine during field testing and FE simulated grid current for the double rotor toroidal winding at rated load with  $v_w = 11$  m/s.

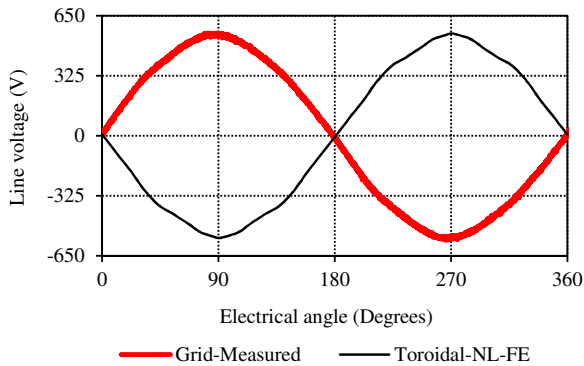


Fig. 11. Measured grid voltage and FE simulated open circuit line voltage for the double rotor toroidal winding PMSG.

circuit line voltage of the double rotor toroidal winding. The non overlap winding injects a much more sinusoidal current waveform into the grid as opposed to the conventional overlap and toroidally wound machines. It is possible to improve the voltage quality with the methods as proposed in [20], which will improve the current fed to the grid. The current waveform can also be improved by adding an external impedance which acts as a buffer between the generator and grid to limit the flow of harmonic currents. The measured and FE simulated efficiency, power factor and reactive power consumption versus load torque of the SL-PMSG case study machine is shown in Figs. 12 and 13 respectively. In these figures positive values

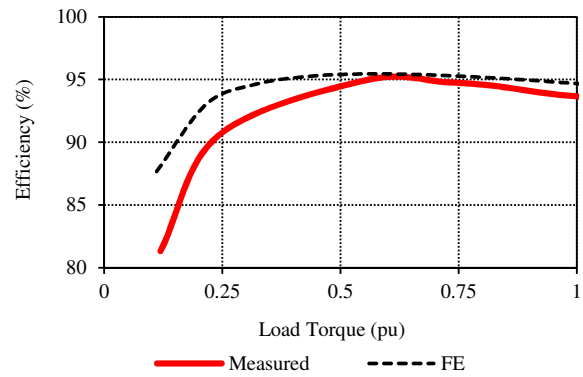


Fig. 12. Measured and FE simulated efficiency versus load torque for the prototype case study SL non overlap winding PMSG.

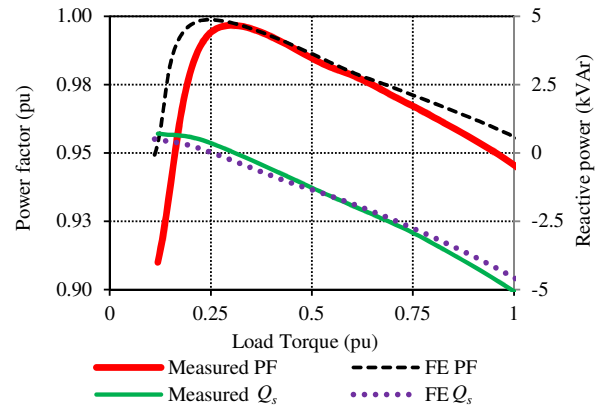


Fig. 13. Measured and FE simulated power factor versus load torque for the prototype case study SL non overlap winding PMSG.

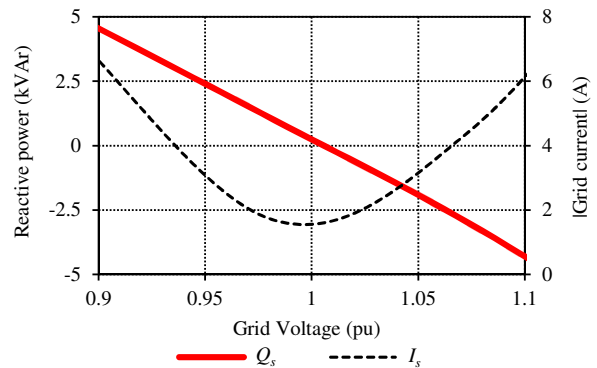


Fig. 14. Measured reactive power and grid current versus p.u. terminal voltage at no load for the case study SL non overlap winding PMSG.

indicate reactive power flowing from the generator to the grid. Fig. 14 shows the effect of varying the terminal voltage of the direct grid PMSG. As specified by the relevant grid code the generator needs to continuously operate in a  $\pm 10\%$  band of the rated grid voltage. For wind farms the grid voltage can be adjusted by means of a central tap changing transformer. Positive reactive power indicates reactive power being delivered to the grid and negative values indicate the absorption of reactive power. This is typically what will happen during low voltage conditions, when the generator will help support the grid voltage.

## VII. CONCLUSION

From the results of this paper it is clear that a different design approach is needed for the directly grid connected PMSG as opposed to conventional PM generator configurations connected to the grid via a power electronic converter. The generator design needs to comply with all the requirements stipulated in the relevant grid codes. A design approach is devised where the generator is optimised with a static FE modelling method coupled with an optimisation algorithm. After verifying the static FE-design with transient FE-analysis, a dynamic modelling procedure is carried out to determine whether the design is suitable for direct grid connection.

In this case the proposed toroidally wound double rotor PMSG is shown to give the best performance regarding active mass and PM content. Due to the much shorter end-windings of this generator it has much better performance than the conventional three phase overlap winding PM generator. The manufacturing of this generator is, however, still a question as it is an unknown concept in direct-drive wind generator design. Furthermore, the induced voltage waveform of this generator can lead to the injection of harmonic currents into the grid. Also the relatively low synchronous reactance leads to high short circuit currents, and unwanted dynamic effects if grid changes occur. The non-overlap SL winding machine is the easiest to manufacture, but has the highest active mass, and the current waveform also has a higher harmonic content than that of the DL non overlap winding.

From this study it seems that for the investigated 15 kW power level the DL non-overlap winding machine is the most favourable topology regarding mass, power quality, direct grid connection and manufacturability. However, it is important to note that for higher power levels, the difference in mass and PM content between the non overlap winding machines and the overlap winding and toroidally wound machines might increase. Due to the low speeds and limits imposed upon the diameters of large electrical wind generators the ratio of torque to diameter does not increase linearly with an increase in power. For wind generators connected to the grid via power electronic converters it might be worthwhile to further investigate the toroidally wound double rotor wind generator, due to its superior performance regarding active and PM mass.

## REFERENCES

- [1] F. Punga and L. Schon, "Der neue kollektorlose Einphasenmotor der Firma Krupp," *Elektrotechnische Zeitschrift*, vol. 47, no. 29, pp. 877–881, 1926.
- [2] B. Hagenkort, T. Hartkopf, A. Binder, and S. Jöckel, "Modelling a direct drive permanent magnet induction machine," in *Proc. of Int. Conf. on Electrical Machines (ICEM'00)*, Espoo, Finland, 2000.
- [3] E. Troster, M. Sperling, and T. Hartkopf, "Finite element analysis of a permanent magnet induction machine," in *International Symposium on Power Electronics, Electrical Drives, Automation and Motion, (SPEEDAM 2006)*, Taormina (Sicily), Italy, 2006.
- [4] A. Thomas, "A doubly-fed permanent magnet generator for wind turbines," Master's thesis, Massachusetts Institute of Technology, 2004.
- [5] R. Vermaak, J. H. J. Potgieter, and M. J. Kamper, "Grid-connected VSC-HVDC wind farm system and control using permanent magnet induction generators," in *IEEE International Conference on Power Electronics and Drive Systems (PEDS)*, Tapei, Taiwan, 2009.
- [6] J. H. J. Potgieter and M. J. Kamper, "Design of new concept gearless direct-grid connected slip-synchronous permanent magnet wind generator," *IEEE Trans. on Industrial Applications*, vol. 48, no. 3, pp. 913–922, 2012.
- [7] —, "Optimum design and technology evaluation of slip permanent magnet generators for wind energy applications," in *IEEE Energy Conversion Congress and Exposition (ECCE)*, Raleigh, NC, USA, 2012.
- [8] H. Polinder, F. F. A. van der Pijl, G. J. de Vilder, and P. Tavner, "Comparison of Direct-Drive and Geared Generator Concepts of Wind Turbines," in *IEEE International Electric Machines & Drives Conference (IEMDC)*, San Antonio, TX, USA, 2005.
- [9] D. Bang, H. Polinder, G. Shrestha, and J. Ferreira, "Promising direct-drive generator system for large wind turbines," in *Wind Power to the Grid - EPE Wind Energy Chapter 1st Seminar, EPE-WECS*, Delft, Netherlands, 2008.
- [10] A. Westlake, J. Bumby, and E. Spooner, "Damping the power-angle oscillations of a permanent-magnet synchronous generator with particular reference to wind turbine applications," *IEE Proc. Electric Power Applications*, vol. 143, no. 3, p. 269, 1996.
- [11] H. Müller, M. Pöller, A. Basteck, M. Tilshcher, and J. Pfister, "Grid compatibility of variable speed wind turbines with directly coupled synchronous generator and hydro-dynamically controlled gearbox," in *Sixth International Workshop on Largescale integration of wind power and transmission networks for offshore wind farms*, Delft, Netherlands, 2006.
- [12] S. Grabic, N. Celanovic, and V. Katic, "Permanent magnet synchronous generator cascade for wind turbine application," *IEEE Trans. on Power Electronics*, vol. 23, no. 3, pp. 1136–1142, 2008.
- [13] "Grid code requirements for wind energy facilities connected to distribution or transmission systems in South Africa," The RSA Grid Code Secretariat, Version 5.4, July, 2012.
- [14] "ELECTRICITY SUPPLY - QUALITY OF SUPPLY, part 2: Voltage characteristics, compatibility levels, limits and assessment methods," Technology Standardization Department (TSD), ESKOM, NRS 048-2:2004, South Africa, 2004.
- [15] "GRID INTERCONNECTION OF EMBEDDED GENERATION, Part 2: Small-scale embedded generation," Technology Standardization Department (TSD), ESKOM, NRS 097-2-1:2010, South Africa, 2010.
- [16] U. Hoffmann, P. Bouwer, and M. J. Kamper, "Direct grid connection of a slip-permanent magnet wind turbine generator," in *Energy Conversion Congress and Exposition (ECCE2011)*, Phoenix, AZ, USA, 2011.
- [17] A. T. Spies and M. J. Kamper, "Reactive power control of a direct grid connected slip synchronous permanent magnet wind generator," in *IEEE International Conference on Industrial Technology (ICIT)*, Cape Town, South Africa, 2013.
- [18] U. Hoffmann and M. J. Kamper, "Low voltage ride-through compensation for a slip-permanent magnet wind turbine generator," in *Southern African Universities Power Engineering Conference (SAUPEC)*, Cape Town, South Africa, 2011.
- [19] J. H. J. Potgieter and M. J. Kamper, "Design considerations in the implementation of an electromagnetic brake for a 15 kW PM wind generator," in *Southern African Universities Power Engineering Conference (SAUPEC)*, Potchefstroom, South Africa, 2013.
- [20] —, "Torque and voltage quality in design optimisation of low cost non-overlap single layer winding permanent magnet wind generator," *IEEE Trans. on Industrial Electronics*, vol. 59, no. 5, pp. 2147–2156, 2012.
- [21] R. Qu and T. Lipo, "Dual-rotor, radial-flux, toroidally wound permanent-magnet machines," *IEEE Trans. on Industry Applications*, vol. 39, no. 6, pp. 1665–1673, 2003.
- [22] Y. Yeh, M. Hsieh, and D. Dorell, "Different arrangements for dual-rotor dual-output radial-flux motors," *IEEE Trans. on Industry Applications*, vol. 48, no. 2, pp. 612–622, 2012.
- [23] J. H. J. Potgieter and M. J. Kamper, "Evaluation of calculation methods and the effects of end-winding inductance on the performance of non-overlap winding PM machines," in *Proc. Int. Conf. on Electrical Machines*, Marseille, France, 2012.
- [24] P. Bouwer, J. H. J. Potgieter, and M. J. Kamper, "Modelling and dynamic performance of a direct-drive direct-grid slip permanent magnet wind generator," in *IEEE International Electric Machines & Drives Conference (IEMDC)*, Niagara Falls, ON, Canada, 2011.